Available online at www.sciencedirect.com

SciVerse ScienceDirect

Solar Energy 86 (2012) 1611–1620

SOLAR ENERGY

www.elsevier.com/locate/solener

# The daily performance of a solar pond integrated with solar collectors

Ismail Bozkurt [a,1], Mehmet Karakilcik [b,*]

[a] *Graduate School of Natural and Applied Sciences, Physics Science Branch, University of Cukurova, Adana 01330, Turkey*

[b] *Department of Physics, Faculty of Arts and Sciences, University of Cukurova, Adana 01330, Turkey*

Received 13 April 2011; received in revised form 30 December 2011; accepted 22 February 2012
Available online 19 March 2012

Communicated by: Associate Editor Aliakbar Akbarzadeh

**Abstract**

The present study deals with heat storage performance investigation of integrated solar pond and collector system. In the experimental work, a cylindrical solar pond system (CSPS) with a radius of 0.80 m and a depth of 2.0 m and four flat plate collectors dimensions of 1.90 m × 0.90 m was built in Cukurova University in Adana, Turkey. The CSPS was filled with salty water of various densities to form three salty water zones (Upper Convective Zone, Non-Convective Zone and Heat Storage Zone). Heat energy collected by collectors was transferred to the solar pond storage zone by using a heat exchanger system which is connected to the solar collectors. Several temperature sensors connected to a data acquisition system were placed vertically inside the CSPS and at the inlet and outlet of the heat exchanger. Experimental studies were performed using 1, 2, 3 and 4 collectors integrated with the CSPS under approximately the same condition. The integrated solar pond efficiencies were calculated experimentally and theoretically according to the number of collectors. As a result, the experimental efficiencies are found to be 21.30%, 23.60%, 24.28% and 26.52%; the theoretical efficiencies to be 23.42%, 25.48%, 26.55% and 27.70% for 1, 2, 3 and 4 collectors, respectively. Theoretical efficiencies were compared with the experimental results and hence a good agreement is found between experimental and theoretical efficiency profiles.


*Keywords:* Solar pond; Solar collector; Integrated system; Heat storage performance; Thermal energy

## 1. Introduction

The energy content of solar radiation can be used as light, heat, and electricity. This diversity makes solar energy an important option to power different energy systems all over the world. Indeed, the interest in solar energy systems has been increasing in recent years throughout the world. This interest has been due to several factors such as the environmental awareness, the effort to minimize countries' dependence on fossil-based, non-renewable fuels, and the international agreements demanding reduction in the greenhouse gases in the earth's atmosphere (Khan et al., 2005). Heat storage technologies, systems and applications are studied in the field of solar energy (Dincer, 1999, 2002). Solar ponds and collectors are very important solar energy systems that generate heat energy from solar energy. Solar ponds are relatively simple devices that operate straightforwardly, require little maintenance (e.g., they need cleaning to maintain water transparency), and have long lifetimes (Dincer and Rosen, 2011). Solar ponds have been studied both theoretically and experimentally since the 1950s (Rivera et al., 2001). Experimental and theoretical temperature distribution and performance analysis were done by Karakilcik et al. (2006a, 2006b). Comparison between theoretical and experimental analysis of a mini solar pond assisted solar still was studied. In this study, effect of sponge cubes in the still, effect of integrating mini solar pond with the still and combination of both were discussed. The average daily production of solar still was found to

* Corresponding author. Tel.: +90 322 3387052; fax: +90 322 3386070.
*E-mail addresses:* ismail_bozkurt44@yahoo.com (I. Bozkurt), kkilcik@cu.edu.tr (M. Karakilcik).

[1] Fax: +90 322 3386070.

0038-092X/$ - see front matter 
doi:10.1016/j.solener.2012.02.025

**Nomenclature**

| | |
|---|---|
| $A$ | surface area ($m^2$) |
| $C$ | specific heat capacity (J/kg °C) |
| CSPS | cylindrical solar pond system |
| $E$ | total solar energy reaching pond (J) |
| $F$ | absorbed energy fraction at a region of $\delta$-thickness |
| $h$ | solar radiation ratio |
| HSZ | heat storage zone |
| $k$ | thermal conductivity (J/m °C h) |
| $L$ | thickness of the layers (m) |
| LCZ | lower convective zone |
| $\dot{m}$ | mass flow (kg/h) |
| $n$ | number of the day |
| NCZ | non-convective zone |
| $Q$ | heat (J) |
| $r$ | radius of the cylindrical solar pond (m) |
| $R$ | thermal resistance of the side and bottom walls (°C/J) |
| $S$ | salinity (g/kg) |
| $T$ | temperature (°C) |
| $U$ | heat transfer coefficient between the ambient air and solar pond (hourly basis) ($MJ/m^2$ °C h) |
| UCZ | upper convective zone |
| $X$ | thickness of inner zones (m) |

*Greek symbols*

| | |
|---|---|
| $\delta$ | thickness where long-wave solar energy is absorbed (m) |
| $\beta$ | incident beam entering rate into water |
| $\gamma$ | latitude angle |
| $\omega$ | hour angle |
| $\theta$ | incident angle |
| $\Phi$ | zenith angle |
| $\varphi$ | tilt angle |
| $\chi$ | beam radiation tilt factor |
| $\rho$ | density ($kg/m^3$) |
| $\Delta x$ | thickness of horizontal layers (m) |

*Subscripts*

| | |
|---|---|
| a | ambient |
| bt | bottom |
| d | declination |
| down | just below zone |
| fpc | flat plate collector |
| I | layer of the pond |
| i | incident |
| in | inner |
| N | number of plate collector |
| out | outer |
| ps | painted metal sheet for first layer |
| p | paint |
| r | reflection |
| s | sheet-iron |
| sc | solar constant |
| ss | sunset |
| sw | side wall |
| solar | solar irradiation inner zones of pond |
| stored | heat stored inner zones of pond |
| th | theoretical |
| up | just above zone |

increase considerably, when it is integrated with a mini solar pond. Theoretical analyses were made using conservation of energy and the results obtained gave very good agreement with the experiments (Velmurugan and Srithar, 2007). An attempt was made to enhance the productivity of the solar stills by connecting a mini solar pond, stepped solar still and a single basin solar still in series. Experiment was also carried out by replacing the single basin solar still into a wick type solar still (Velmurugan et al., 2009).

A lot of studies have been done about solar pond and collectors (Smyth et al., 2006; Karakilcik and Dincer, 2008; Anderson et al., 2010; Alvarez et al., 2010; Karim et al., 2010, 2011; Kumar and Rosen, 2011; Moghadam et al., 2011). Some experimental and theoretical studies dealt with a solar pond integrated with different applications to increase performance of the solar pond (Velmurugan and Srithar, 2007; Velmurugan et al., 2009; Akbarzadeh et al., 2009; El-Sebaii, 2005; El-Sebaii et al., 2008; Singh et al., 2011). But integrating solar pond with collector system has not been studied anywhere. To increase solar pond performance solar pond and collectors were used together. Solar ponds and collectors have some advantages and disadvantages. It is known that stored heat energy by solar collectors is lost if it is not used in few days. On the other hand solar pond heats up slowly but store heat in a longer period of time than solar collectors. In this study, integrated system that is a combination of a solar pond and collectors is used. Heat energy obtained from solar collector is transferred to the solar pond storage zone through a heat exchanger system that is placed in storage zone.

In this work, an integrated solar pond and collector system were constructed at the Space Sciences and Solar Energy Research and Application Center (UZAYMER), Cukurova University in Adana, Turkey (i.e., 35°18′ $E$ longitude, 37°05′ $N$ latitude). Experiments were done to determine heat storage, and the efficiencies of the heat storage zone for a particular rate of incident solar radiation and heat energy transferred from solar collectors. The data allow heat storage zone performance to be obtained experimentally in sunny days in September. Energy balance equations of the zones were derived to determine energy storage in the pond and hence efficiencies. Some significant parameters, such as heat capacity as function of the salinity of the salty water layers, temperatures, average flow rate and the thicknesses of zones were also investigated.

## 2. Experimental apparatus and procedure

Integrated system is a new combination of a solar pond and collectors.

### 2.1. Solar ponds

Solar ponds are composed of three zones. The first zone, Upper Convective Zone (UCZ), is the fresh water layer at the top of the pond. This zone is fed with fresh water in order to maintain its density close to the density of fresh water and to replenish the lost water due to evaporation. The second zone is Non-Convective Zone (NCZ) between the Lower Convective Zone (LCZ) and the UCZ. NCZ is composed of salty water layers whose brine density gradually increases towards LCZ. NCZ is the key to a functional solar pond. It allows solar radiation to penetrate into the storage zone while cost-effective method of collecting and storing heat is done in the LCZ because water is opaque to infrared radiation. The third zone is known as the Lower Convective Zone (LCZ) (so-called as the Heat Storage Zone, HSZ) and it is composed of salty water with highest density. Considerable part of the solar energy is absorbed and stored by this bottom region.

### 2.2. Integrated system

For the experimental work, an integrated system which is consist of cylindrical solar pond with a radius of 0.80 m and a depth of 2 m and solar collectors was built in Cukurova University in Adana, Turkey (Fig. 1a). Fig. 1a shows a schematic representation of an integrated system, consisting of the cylindric solar pond, heat exchanger and solar collectors. Fig. 1b and c shows a photo of the integrated solar pond and the heat exchanger system in the HSZ. In Fig. 1a, $X_1$ is the distance from bottom of the UCZ to the surface, $X_2$ is the distance from bottom of the NCZ to the surface, $X_3$ is the distance from bottom of the HSZ to the surface, $N$ is the number of collectors. The experimental temperature distributions were measured using temperature sensors, which were placed into the inner zones and inlet and outlet of the heat exchanger. Hence the temperature distribution profiles of these regions at any time were experimentally obtained by a data acquisition system. To measure the temperature distributions of various regions, the temperature sensors were placed into the inner zones, starting from the bottom, at 0.10, 0.30, 0.50, 0.70, 0.90, 1.10, 1.30, 1.50, 1.70, 1.90 m heights, The data acquisition system was connected to a computer for data recording, monitoring and processing. The solar energy data is obtained using a pyranometer, and hourly and daily average air temperatures are obtained from a local meteorological station.

## 3. Salt gradient protection system

The density gradient in the NCZ is very important to keep the stored energy. In order to maintain the density gradient of the pond an auxiliary operating system on a feedback principle was developed. It generated a continuous and self regulating operation. This was a passive system based on the natural circulation of water caused by density difference, as it was first proposed by Akbarzadeh and MacDonald (1982). Similar protection system was used successfully by Karakilcik (1998) and Bozkurt (2006). It is a cylindrical polyethylene tank having 1.20 m length and 0.30 m diameter. The tank has a connection from its bottom to the top of the HSZ. Because of the density difference between the storage zone and a higher zone, the less dense brine entered via a plastic tube to the top of the tank from top of the NCZ and diffused through a salt bed on a mesh within the tank and reached about 1180–1200 kg/m$^3$ density at the bottom. This more dense brine was injected into the top level of the HSZ via a distributing pipe system. The salty water distribution system was made of polyethylene tubes and in circular form with a diameter of 1.20 m and the pipe has 0.02 m diameter, and several holes along them led the higher density brine out, and sited horizontally at the top of the HSZ.

## 4. Heat storage performance analysis

Solar energy is collected by solar pond and collectors. Solar energy is reached from the sun reaches the pond and collector surface by the sunlight. The sunlight which reaches the bottom of the pond, remains entrapped and stored there, while the sunlight which reaches the surface of the collector is converted into heat energy. Heat energy produced by collectors are transferred to the solar pond's storage zone by using a heat exchanger system. The useful thermal energy is then withdrawn from the solar pond bottom in the form of hot water.

### 4.1. Energy balance equation for HSZ

The general energy balance for the HSZ of the integrated solar pond and collector system can be written as:

$$Q_{\mathrm{HSZ}} = Q_{\mathrm{u,fpc}} + Q_{\mathrm{HSZ,solar}} - Q_{\mathrm{bt}} - Q_{\mathrm{up}} - Q_{\mathrm{sw}} \tag{1}$$

where $Q_{\mathrm{HSZ}}$ is heat stored in the HSZ, $Q_{\mathrm{u,fpc}}$ is the useful heat gain by the flat plate collector, $Q_{\mathrm{HSZ,solar}}$ is amount of the solar radiation entering the HSZ which is transmitted from the NCZ after attenuation of incident solar radiation in the NCZ, $Q_{\mathrm{bt}}$ is the heat loss from the bottom of the pond, $Q_{\mathrm{up}}$ is the heat loss from the HSZ to the NCZ, $Q_{\mathrm{sw}}$ is the heat loss from the side wall.

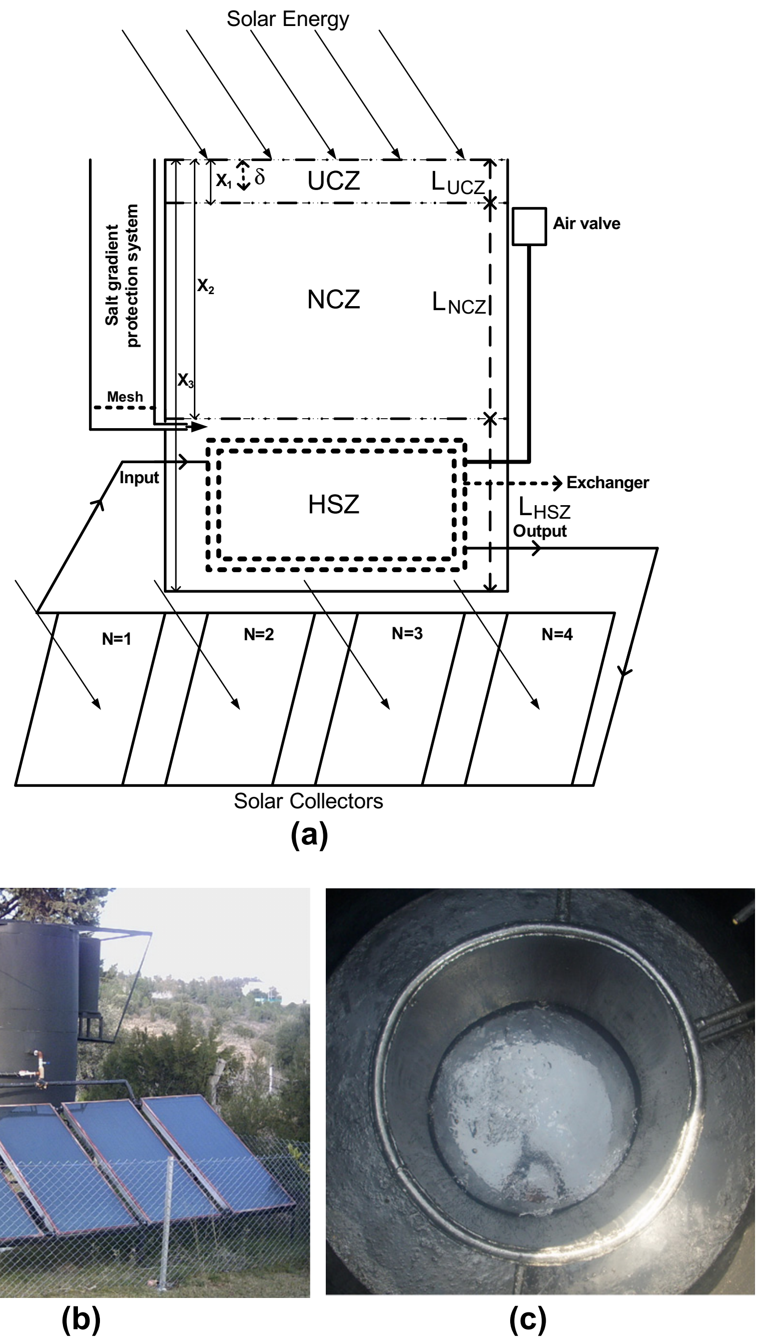


Fig. 1. (a) A schematic view of the integrated solar pond. (b) A photo of the integrated solar pond. (c) A photo of the heat exchanger system in the HSZ.

$$Q_{u,fpc} = \dot{m}C(T_{out} - T_{in}) \tag{2}$$

$$Q_{HSZ,solar} = \beta E A_{HSZ}[(1 - F)h(x_3 - \delta)] \tag{3}$$

$$Q_{bt} = AR_{ps}(T_{bt} - T_a) \tag{4}$$

$$Q_{up} = \frac{kA}{\Delta x}(T_{HSZ} - T_{NCZ}) \tag{5}$$

$$Q_{sw} = \frac{2\pi L_{HSZ} R_{ps}}{\ln\left(\frac{r_{out}}{r_{in}}\right)}(T_{HSZ} - T_a) \tag{6}$$

Thus, the heat balance can be written as:

$$\begin{aligned} Q_{HSZ} = {} & \dot{m}C(T_{out} - T_{in}) + \beta E A_{HSZ}[(1 - F)h(x_3 - \delta)] \\ & - AR_{ps}(T_{bt} - T_a) - \frac{kA}{\Delta x}(T_{HSZ} - T_{NCZ}) \\ & - \frac{2\pi L_{HSZ} R_{ps}}{\ln\left(\frac{r_{out}}{r_{in}}\right)}(T_{HSZ} - T_a) \end{aligned} \tag{7}$$

where $\dot{m}$ is the water mass flow rate in the collectors, $C$ is the specific heat capacity, $T_{in}$ is the temperature of the collector inlet, $T_{out}$ is the temperature of the collector outlet, $\beta$ is the fraction of incident beam entering into the CSPS, $E$ is the total solar energy reaching the pond surface,

$A_{HSZ}$ is the sunny area of HSZ, $F$ is absorbed energy fraction at a region of $\delta$ thickness, h is the solar radiation ratio, $A$ is the surface area of the pond, $T_a$ is the ambient air temperature, $R_{ps}$ is the thermal resistance of the painted metal sheet bottom and side walls, k is the thermal conductivity of salty water, $L_{HSZ}$ is the thickness of HSZ ($X_3$–$X_2$) (m), $r_{in}$ and $r_{out}$ are inner and outer radius of the cylindrical solar pond.

The specific heat capacity of the solar pond zones are calculated using empirical Eq. (8) (Sun et al., 2008).

$$C = (-0.0044S + 4.1569)1000 \tag{8}$$

where $S$ is the salinity. The salinity is given by

$$S = \frac{(\rho - 998.24)}{0.756} \tag{9}$$

where $\rho$ is the salty water density. $\beta$ is the fraction of the incident solar incident that actually enters the pond (Hawlader, 1980):

$$\beta = 1 - 0.6\left[\frac{\sin\theta_i - \sin\theta_r}{\sin\theta_i + \sin\theta_r}\right]^2 - 0.4\left[\frac{\tan\theta_i - \tan\theta_r}{\tan\theta_i + \tan\theta_r}\right]^2 \tag{10}$$

where $\theta_i$ and $\theta_r$ are the incidence angle and the refraction angle. $h$ is representing the ratio of the solar energy reaching the bottom of the layer I is given by Bryant and Colbeck (1997) as:

$$h_I = 0.727 - 0.056\ln\left[\frac{(x_I - \delta)}{\cos\theta_r}\right] \tag{11}$$

where $x_I$ is the thickness of the layer $I$ which varies from 1 to 3 for UCZ, NCZ and HSZ. $\delta$; thickness of the layer in the UCZ where long-wave solar energy is absorbed. $R_{ps}$ is the thermal resistance of the painted metal sheet surrounding the first layer, respectively as:

$$R_{ps} = \frac{k_p k_s}{S_p k_s + S_s k_p} \tag{12}$$

where $k_p$ and $k_s$ are thermal conductivities of the paint and iron-sheet, and $S_p$ and $S_s$ are the corresponding thicknesses.

### 4.2. Energy balance equation for NCZ

The solar radiation incident on the surface of the NCZ, which is the part of the incident solar radiation on the surface of the pond, is transmitted from the UCZ. A small fraction of the incident solar radiation on the NCZ is reflected from the NCZ to the UCZ. The reflected part of the incident solar radiation increases the UCZ efficiency. Part of the incident solar radiation is transmitted to the HSZ while part of the incident solar radiation is absorbed by the NCZ. We can write the energy balance for the NCZ as:

$$Q_{NCZ} = Q_{NCZ,solar} + Q_{down} - Q_{up} - Q_{sw} \tag{13}$$

where $Q_{NCZ}$ is the heat stored energy in the NCZ, $Q_{NCZ,solar}$ is amount of the solar radiation entering the NCZ which is transmitted from the UCZ after attenuation of incident solar radiation in the UCZ, $Q_{down}$ is the heat transferred from the bottom of the pond, $Q_{up}$ is the heat loss from the NCZ to the upper zone, $Q_{sw}$ is the heat loss to the side wall.

$$Q_{NCZ,solar} = \beta E A_{NCZ}[(1 - F)h(x_2 - \delta)] \tag{14}$$

$$Q_{down} = \frac{kA}{\Delta x}(T_{HSZ} - T_{NCZ}) \tag{15}$$

$$Q_{up} = \frac{kA}{\Delta x}(T_{NCZ} - T_{UCZ}) \tag{16}$$

$$Q_{sw} = \frac{2\pi L_{NCZ} R_{ps}}{\ln\left(\frac{r_{out}}{r_{in}}\right)}(T_{NCZ} - T_a) \tag{17}$$

Thus, the heat balance can be written as;

$$Q_{NCZ} = \beta E A_{NCZ}[(1 - F)h(x_2 - \delta)] + \frac{kA}{\Delta X}(T_{HSZ} - T_{NCZ}) - \frac{kA}{\Delta x}(T_{NCZ} - T_{UCZ}) - \frac{2\pi L_{NCZ} R_{ps}}{\ln\left(\frac{r_{out}}{r_{in}}\right)} \times (T_{NCZ} - T_a) \tag{18}$$

where $A_{NCZ}$ is sunny area of NCZ, $T_{NCZ}$ is average temperature of the NCZ, $T_{UCZ}$ is average temperature of the UCZ, $L_{NCZ}$ is the thickness of NCZ ($X_2$–$X_1$). NCZ is composed of salty water layers. The average temperature $T_{NCZ}$ is calculated using the salty water layers' temperatures.

### 4.3. Energy balance equation for UCZ

Part of the incident solar radiation is transferred from the UCZ surface to air. Part of the incident solar radiation is transmitted from the UCZ to the NCZ and rest of the incident solar radiation is absorbed in the zone. We can write the energy balance for the UCZ as:

$$Q_{UCZ} = Q_{UCZ,solar} + Q_{down} - Q_{up} - Q_{sw} \tag{19}$$

where $Q_{UCZ}$ is the heat stored energy in the NCZ, $Q_{UCZ,solar}$ is amount of the solar radiation entering the UCZ from surface of the pond.

$$Q_{UCZ,solar} = \beta E A_{UCZ}[1 - (1 - F)h(x_1 - \delta)] \tag{20}$$

$$Q_{down} = \frac{kA}{\Delta x}(T_{NCZ} - T_{UCZ}) \tag{21}$$

$$Q_{up} = UA(T_{UCZ} - T_a) \tag{22}$$

$$Q_{sw} = \frac{2\pi L_{UCZ} R_{ps}}{\ln\left(\frac{r_{out}}{r_{in}}\right)}(T_{UCZ} - T_a) \tag{23}$$

Thus, the heat balance can be written as:

$$Q_{UCZ} = \beta E A_{UCZ}[1 - (1 - F)h(x_1 - \delta)] + \frac{kA}{\Delta X}(T_{NCZ} - T_{UCZ}) - UA(T_{UCZ} - T_a) - \frac{2\pi L_{UCZ} R_{ps}}{\ln\left(\frac{r_{out}}{r_{in}}\right)}(T_{UCZ} - T_a) \tag{24}$$

where $A_{UCZ}$ is sunny area of UCZ ($m^2$), $U$ is heat transfer coefficient between the ambient air and solar pond and

$L_{UCZ}$ is the thickness of UCZ ($X_1$). The energy efficiency of the integrated solar pond and collector system is given as:

$$\eta_{exp} = \frac{Q_{stored}}{Q_{fpc,solar} + Q_{solar}} \tag{25}$$

where $Q_{stored}$ is the net heat stored energy in the solar pond, $Q_{solar}$ is the solar energy reaching the pond surface. $Q_{fpc,solar}$ is the incident solar energy of the absorber flat plate surface and it is given as:

$$Q_{fpc,solar} = E(\tau\alpha)A^{N}_{fpc} \tag{26}$$

where $A^{N}_{fpc}$ is the collector area, $\tau$ is the transmission coefficient of the collector surface and $\alpha$ is the emissivity of the absorber surface of the flat plate collector.

The efficiency of the integrated solar pond was calculated by using theoretical data:

$$\eta_{th} = \frac{Q_{th,stored}}{Q_{th,fpc,solar} + Q_{th,solar}} \tag{27}$$

where $Q_{th,solar}$ were calculated theoretically by using Eqs. (7), (18), and (24). $E_{th,solar}$ and $Q_{th,fpc,solar}$ were determined for horizontal surface and tilt surface as given as (Kalogirou, 2009):

$$E_{th,solar} = \frac{86400G_{sc}}{\pi}\left[1+0.033\cos\left(\frac{360n}{365}\right)\right]\left[\cos(\gamma)\cos(\delta_d)\sin(\omega_{ss}) + \left(\frac{\pi\omega_{ss}}{180}\right)\sin(\gamma)\sin(\delta_d)\right] \tag{28}$$

where $G_{sc}$ is the solar constant, $n$ is the number of day, $\gamma$ is the latitude angle, $\delta_d$ is the declination angle, $\omega_{ss}$ is the sunset hour in degrees.

$$Q_{th,fpc,solar} = (\chi)E_{th,solar}A^{N}_{fpc} \tag{29}$$

where $\chi$ is called the beam radiation tilt factor for south-facing tilted surface and it is given as:

$$\chi = \frac{\cos(\theta)}{\cos(\Phi)} = \frac{\sin(\gamma-\varphi)\sin(\delta_d) + \cos(\gamma-\varphi)\cos(\delta_d)\cos(\omega)}{\sin(\gamma)\sin(\delta_d) + \cos(\gamma)\cos(\delta_d)\cos(\omega)} \tag{30}$$

where $\theta$ is the incident angle, $\Phi$ is the zenith angle, $\varphi$ is the tilt angle and ω is the hour angle.

## 5. Results and discussion

Here we now present the results of the energy efficiencies depend on the number of collectors and compare these results to show the affect of the collectors. It has been demonstrated that the stability of the salt density distribution in a solar pond is of great significance as shown in Table 1. It lists the variations of the experimental salty water densities for inner zones of the integrating solar pond according to the number of collectors (e.g., 1, 2, 3 and 4 collectors). Especially, some slight effect of the number of collectors are seen on stability of the NCZ and HSZ. The primary reason of the density differences are increase of the inner zone temperature due to especially increase in heat storage zone temperature by using collectors. As we know that the salt diffusion in the inner zones of the solar pond is increased by temperature. These changes can be eliminated by adding fresh water to the top of the pond and to keep under control the density gradient, the highest density salty water is added to the top of the HSZ by using salt gradient protection system, continuously.

Fig. 2 shows the variations of the experimental salty water densities with the height from the bottom of the pond in various months (e.g. June, July, August, September, October, November and December). Here, some slight differences are observed between the density variation measured of the pond's layers for different months, due to exchange of the temperatures of the inner zones and diffusion of the flow rate of salt molecules. The primary reason of differences might be the increase in temperature in summer. This change mostly originates from the thermophysical property of the salty water.

The density distribution is kept approximately stable by using salt gradient protection system. The variations of the experimentally measured salty water densities with respect to the height measured from the bottom of the integrated solar pond throughout the year were given in Table 2. As seen Table 2, the density gradient of the NCZ was stable. The corrosion of the density gradient was compensated by using salt gradient system effectively. So, the life time of the solar pond is not effected negatively.

Non-integrated a cylindrical solar pond was used to store the heat energy in the first experiment. The experimental temperature measurements taken from the pond. Fig. 4 shows average experimental temperature distributions measured inside pond during days in the months of June, July and August. These experimental temperatures were in fact measured on hourly basis. As shown in Fig. 4 the maximum average temperature of the HSZ is 43.32 °C. The reasons of the low temperature in the HSZ are that small surface area, shading by the side vertical walls, heat losses and turbidity in the inner zones. So, the reaching solar energy of the HSZ is decreased by these negative effects.

In the second experiment, the integrated solar pond system is used to store much more heat energy. As a result, the HSZ of the conventional solar pond stores much more thermal energy if flat plate collectors are used depend on the number of collectors. The experimental temperature measurements were taken from integrated system on September in our system. Solar collectors were used to increase temperature of the HSZ. Experimental studies were performed using 1, 2, 3 and 4 collectors under approximately the same condition. One collector was used and temperature measurements were recorded from 09.00 to 17.00. To ensure approximately the same conditions HSZ was cooled to the starting temperature using cold water through heat exchanger system.

After obtaining approximately the same conditions the next day two collectors were used and also similar experiments were done for three and four collectors. Results are shown in Figs. 5–8.

Table 1
Density distribution of the solar pond zones (kg/m$^3$), (Using one, two, three and four collectors).

| Height (m) | HSZ | | | | | NCZ | | | | UCZ |
|---|---|---|---|---|---|---|---|---|---|---|
| | 0.10 | 0.30 | 0.50 | 0.70 | 0.90 | 1.10 | 1.30 | 1.50 | 1.70 | 1.90 |
| $N=1$ | | | | | | | | | | |
| 09.00 | 1181 | 1181 | 1180 | 1180 | 1170 | 1148 | 1104 | 1060 | 1022 | 1005 |
| 13.00 | 1181 | 1180 | 1180 | 1179 | 1170 | 1146 | 1105 | 1060 | 1023 | 1005 |
| 17.00 | 1181 | 1180 | 1180 | 1177 | 1169 | 1145 | 1105 | 1060 | 1024 | 1006 |
| $N=2$ | | | | | | | | | | |
| 09.00 | 1182 | 1180 | 1180 | 1180 | 1170 | 1149 | 1105 | 1060 | 1022 | 1004 |
| 13.00 | 1180 | 1180 | 1180 | 1178 | 1169 | 1149 | 1105 | 1060 | 1023 | 1005 |
| 17.00 | 1180 | 1180 | 1180 | 1178 | 1169 | 1148 | 1105 | 1060 | 1023 | 1005 |
| $N=3$ | | | | | | | | | | |
| 09.00 | 1182 | 1181 | 1181 | 1180 | 1172 | 1150 | 1105 | 1060 | 1023 | 1002 |
| 13.00 | 1180 | 1180 | 1179 | 1179 | 1171 | 1149 | 1106 | 1061 | 1024 | 1002 |
| 17.00 | 1181 | 1180 | 1179 | 1179 | 1170 | 1149 | 1106 | 1062 | 1024 | 1003 |
| $N=4$ | | | | | | | | | | |
| 09.00 | 1181 | 1181 | 1180 | 1180 | 1170 | 1148 | 1103 | 1060 | 1022 | 1003 |
| 13.00 | 1180 | 1179 | 1179 | 1177 | 1169 | 1149 | 1104 | 1060 | 1023 | 1004 |
| 17.00 | 1180 | 1178 | 1178 | 1175 | 1169 | 1148 | 1105 | 1060 | 1024 | 1005 |

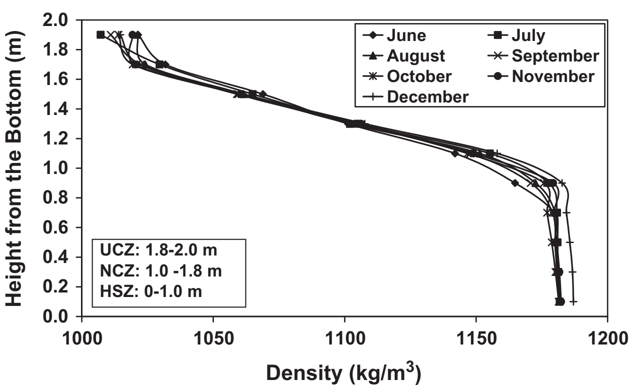


Fig. 2. Density distribution of the solar pond.

The density and salinity differences are important parameter to calculate energy distribution at the low temperature in the solar pond. So, we used the empirical Eqs. (8) and (9) in Section 4 to calculate our solar pond zones' salinity differences and the specific heat capacity at low temperature in Figs. 9 and 10.

The energy stored for each zone was determined by calculating the temperature differences for daily profiles for each number of collectors. In order to determine the energy stored for the inner zones the experimental temperature distribution have been obtained (see Fig. 5–8). It was determined by using Eqs. (7), (18), and (24) in Section 4. These are seen in Fig. 11 for using 1, 2, 3 and 4 collectors. The energy stored in HSZ to be 16.14, 23.30, 34.84 and 49.84 MJ. Similarly, the energy stored in the NCZ to be 9.01, 11.78, 13.70 and 19.77 MJ, while the energy stored in the UCZ to be 4.04, 4.39, 7.23 and 7.38 MJ, respectively. The transferred useful heat energy from the flat plate collectors was calculated by using Eq. (2) for using 1, 2, 3 and 4. The solar energy data is obtained using a pyranometer from a local meteorological station. The monthly total global solar radiation is given in Fig. 3.

Table 2
Density distrubution of the integrated solar pond zones for a year (kg/m$^3$).

| Height (m) | HSZ | | | | | NCZ | | | | UCZ |
|---|---|---|---|---|---|---|---|---|---|---|
| | 0.10 | 0.30 | 0.50 | 0.70 | 0.90 | 1.10 | 1.30 | 1.50 | 1.70 | 1.90 |
| September | 1190 | 1189 | 1188 | 1187 | 1187 | 1156 | 1109 | 1060 | 1023 | 1012 |
| October | 1188 | 1188 | 1187 | 1186 | 1186 | 1156 | 1106 | 1061 | 1025 | 1015 |
| November | 1185 | 1183 | 1183 | 1182 | 1181 | 1157 | 1102 | 1061 | 1030 | 1016 |
| December | 1181 | 1181 | 1175 | 1174 | 1173 | 1154 | 1102 | 1061 | 1029 | 1021 |
| January | 1185 | 1183 | 1182 | 1181 | 1163 | 1144 | 1103 | 1069 | 1038 | 1008 |
| February | 1182 | 1181 | 1180 | 1179 | 1164 | 1142 | 1101 | 1068 | 1031 | 1021 |
| March | 1181 | 1181 | 1181 | 1180 | 1177 | 1155 | 1104 | 1065 | 1029 | 1007 |
| April | 1181 | 1180 | 1180 | 1180 | 1172 | 1151 | 1102 | 1061 | 1024 | 1021 |
| May | 1181 | 1180 | 1180 | 1179 | 1170 | 1147 | 1103 | 1059 | 1022 | 1011 |
| June | 1181 | 1180 | 1178 | 1177 | 1175 | 1146 | 1105 | 1059 | 1019 | 1014 |
| July | 1182 | 1181 | 1180 | 1179 | 1179 | 1149 | 1106 | 1060 | 1020 | 1019 |
| August | 1187 | 1186 | 1185 | 1184 | 1182 | 1158 | 1107 | 1061 | 1022 | 1014 |

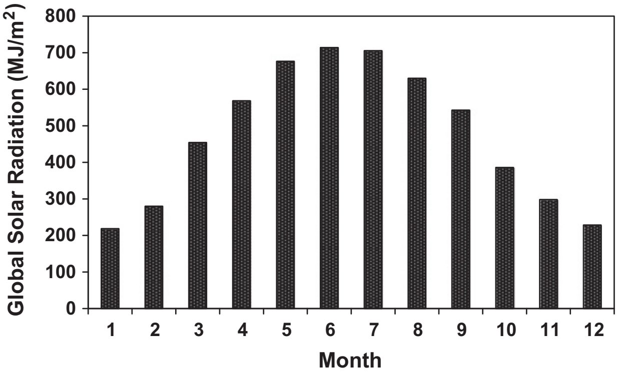


Fig. 3. The monthly total global solar radiation in Adana, Turkey (Adana Meteorology Regional Offices, 2010).

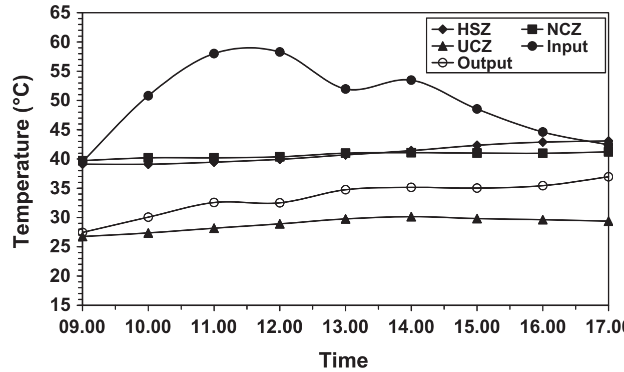


Fig. 6. Average temperature distribution in the solar pond zones and at inlet and outlet of the heat exchanger system (using two collectors).

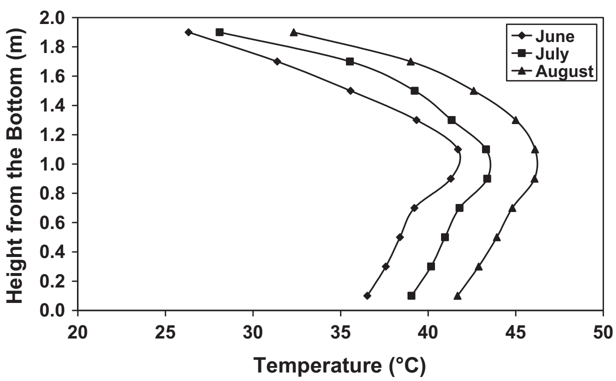


Fig. 4. Temprature distribution of the solar pond.

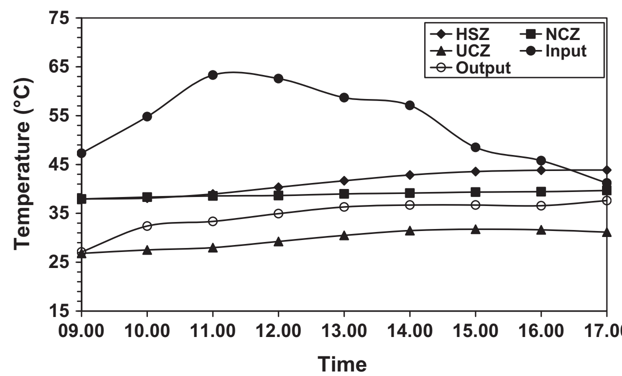


Fig. 7. Average temperature distribution in the solar pond zones and at inlet and outlet of the heat exchanger system (using three collectors).

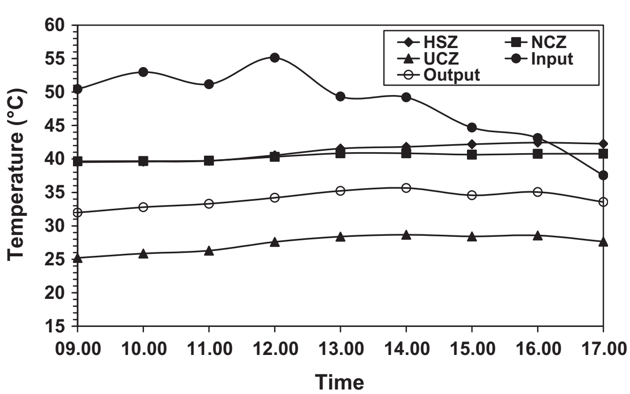


Fig. 5. Average temperature distribution in the solar pond zones and at inlet and outlet of the heat exchanger system (using one collector).

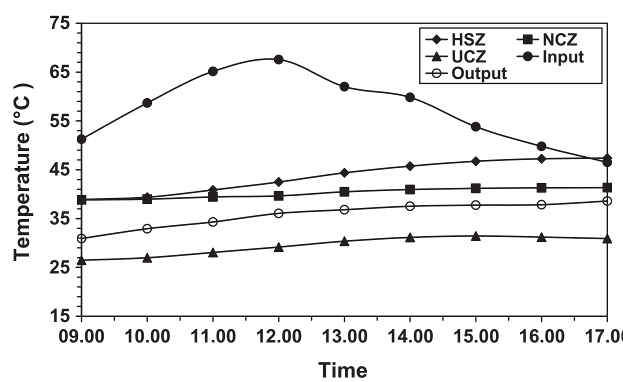


Fig. 8. Average temperature distribution in the solar pond zones and at inlet and outlet of the heat exchanger system (using four collectors).

In a solar pond, efficiencies are low since the stored energy is much smaller than the incident solar radiation on the zone surfaces. The stored heat energy by solar collectors is lost if it is not used in few days. On the other hand solar pond heats up slowly but store heat in a longer period of time than solar collectors. To increase performance of the solar pond, solar collectors are used. Heat energy obtained from solar collector is transferred to the solar pond storage zone through a heat exchanger system that is placed in storage zone. The performance of the integrated solar pond depends upon the total radiation reaching its zones and collector's surface. The integrated solar pond efficiencies are calculated experimentally and theoretically by using Eqs. (25)–(27) according to the number of collectors. As seen in Fig. 12 the experimental efficiency to be 21.30%, 23.60%, 24.28% and 26.52% for 1, 2, 3 and 4 collectors, respectively. The theoretical efficiency to be 23.42%, 25.48%, 26.55% and 27.70% for 1, 2, 3 and 4 collectors, respectively. Theoretical efficiencies are compared with the experimental results and hence a good agreement

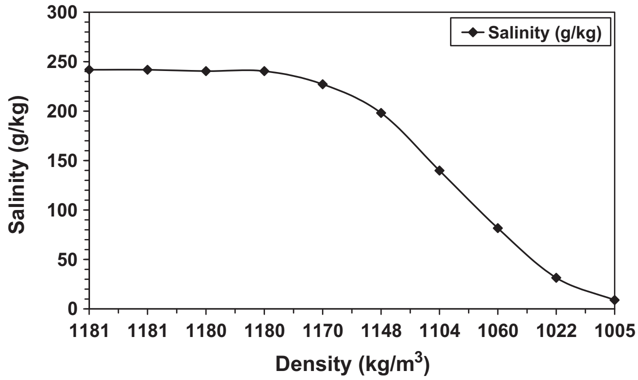


Fig. 9. Change of salinity according to the density of the solar pond zones.

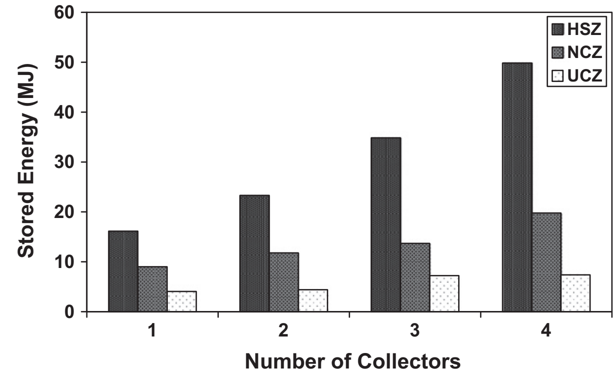


Fig. 11. Stored energy in the solar pond zones according to number of collectors.

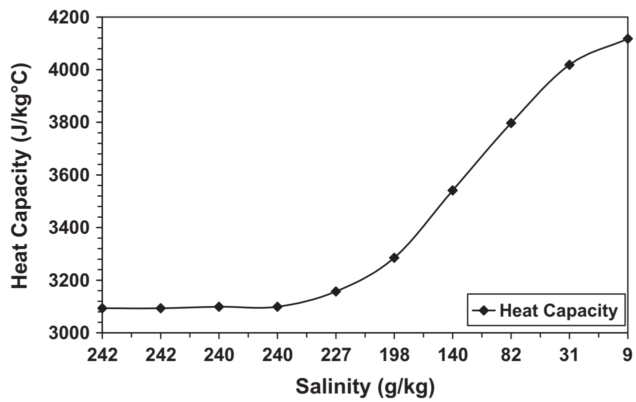


Fig. 10. Heat capacity of the solar pond.

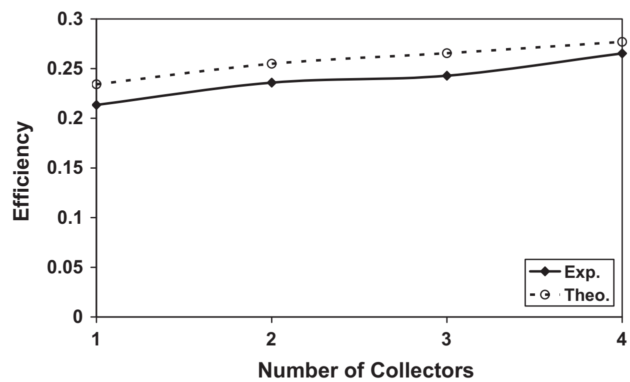


Fig. 12. Energy efficiency of the solar pond according to the number of collectors.

is found between experimental and theoretical efficiency profiles. Number of collectors has an important effect on performance of the solar pond. Increasing shading area from the top to the bottom of the pond allows less solar radiation to pass through and decreases the thermal potential of the pond and hence its performance. We analyze the energy efficiency of solar pond to investigate the performance. The maximum efficiencies of the solar pond are seen to occur for using four collectors.

The energy efficiency of the pond is decreased because of heat energy losses due to thermal transfer from the UCZ to air. A low fraction of the incident solar radiation is stored in the pond and the UCZ efficiency is negligible especially compared to that of the NCZ. The NCZ efficiency consequently has a greater effect on the performance of the pond. Most of the energy is stored in the HSZ of the pond.

As a result, the HSZ of the solar pond stores more thermal energy if collectors are used. The considerable temperature differences between the zones according to the number of collectors. Number of collectors significantly affect the thermal performance of the pond. We thus suggest that heat storage, number of collectors, heat losses, shading areas and solar radiation absorption should be carefully considered when determining the thermal performance of solar ponds.

## 6. Conclusions

Heat storage performance investigation of the integrated solar pond and collector system has been investigated. Efficiencies of the solar pond have been expressed by using energy balance equations for 1, 2, 3 and 4 collectors. The results show that pond performance is affected strongly by the number of collectors. The sunny area of the pond and collector numbers and flow rate of the water from inlet and outlet temperature of the exchanger are very sensitive the amount of the incident solar energy. The temperature of the pond is suddenly increase in top layer of the HSZ and bottom layer of the NCZ, but the salt diffusion is negligibly small because of the feedback with high density saline water by salt gradient system which is worked well. So, to increase the integrated solar pond system performance, the zone thicknesses and sunny area, collector number and the salt gradient system should be modified to achieve higher efficiency and stability of the pond. Through careful design parameter modifications and the other solar energy systems (i.e., solar collector) pond performance can be maintained even if the incoming solar radiation reaching the zones is increased. It is shown that the collectors provides many conveniences in calculating the heat storage efficiency in the integrated system, and in determining the relations with heat loads and a best operating state. Here, we carried out efficiency calculations of integrated solar pond experimentally and theoretically in order to demonstrate the effect of collectors on the performance of the insulated cylindrical solar pond. Therefore, the energy efficiency of the integrated solar pond is an important parameter in practical applications.

## Acknowledgement

The authors are thankful to University of Cukurova for financial support of the present work (Grant No. FEF2004 BAP4, FEF2009D2, and FEF2010BAP5).

## References

Adana Meteorology Regional Offices, 2010. Turkish State Meteorological Service, Ankara, Turkey.

Akbarzadeh, A., MacDonald, R.W.G., 1982. Introduction of a passive method for salt replenishment in the operation of the solar ponds. Solar Energy 29, 71–76.

Akbarzadeh, A., Johnson, P., Singh, R., 2009. Examining potential benefits of combining a chimney with a salinity gradient solar pond for production of power in salt affected areas'. Solar Energy 83, 1345–1359.

Alvarez, A., Cabeza, O., Muñiz, M.C., Varela, L.M., 2010. Experimental and numerical investigation of a flat-plate solar collector. Energy 35, 3707–3716.

Anderson, T.N., Duke, M., Carson, J.K., 2010. The effect of colour on the thermal performance of building integrated solar collectors. Solar Energy Materials & Solar Cells 94, 350–354.

Bozkurt, I., 2006. Performance Investigation of having an Insulation and Cover Cylindrical Model Solar Pond. MSc. Thesis. Cukurova University, Adana, Turkey, (in Turkish).

Bryant, H.C., Colbeck, I., 1997. A solar pond for London. Solar Energy 19, 321.

Dincer, I., 1999. Evaluation and selection of energy storage systems for solar thermal applications. International Journal of Energy Research 23, 1017–1028.

Dincer, I., 2002. Thermal energy storage systems as a key technology in energy conservation. International Journal of Energy Research 26, 567–588.

Dincer, I., Rosen M.A., 2011. Thermal Energy Storage Systems and Applications, Wiley, New York. ISBN:978-0-470-74706-3.

El-Sebaii, A.A., 2005. Thermal performance of a shallow solar-pond integrated with a baffle plate. Applied Energy 81, 33–53.

El-Sebaii, A.A., Ramadan, M.R.I., Aboul-Enein, S., Salem, N., 2008. Thermal performance of a single-basin solar still integrated with a shallow solar pond. Energy Conversion and Management 49, 2839–2848.

Hawlader, M.N.A., 1980. The influence of the extinction coefficient on the effectiveness of solar ponds. Solar Energy 25, 461–464.

Kalogirou, 2009. Solar Energy Engineering Processes and Systems. Cyprus University of Technology, ISBN 13:978-0-12-374501-9.

Karakilcik, M., 1998. Determination of the Performance of an Insulated Prototype Solar Pond. Ph.D. Thesis. Cukurova University, Adana, Turkey (in Turkish).

Karakilcik, M., Kıymac, K., Dincer, I., 2006a. Experimental and theoretical temperature distributions in a solar pond. International Journal of Heat and Mass Transfer 49, 825–835.

Karakilcik, M., Dincer, I., Rosen, M.A., 2006b. Performance investigation of a solar pond. Applied Thermal Engineering 26, 727–735.

Karakilcik, M., Dincer, I., 2008. Exergetic performance analysis of a solar pond. International Journal of Thermal Sciences 47, 93–102.

Karim, C., Slim, Z., Kais, C., Jomaa, S.M., Akbarzadeh, A., 2010. Experimental study of the salt gradient solar pond stability. Solar Energy 84, 24–31.

Karim, C., Jomaa, S.M., Akbarzadeh, A., 2011. A laboratory experimental study of mixing the solar pond gradient zone. Solar Energy 85, 404–417.

Khan, F.I., Hawboldt, K., Iqbal, M.T., 2005. Life cycle analysis of wind–fuel cell integrated system. Renewable Energy 30, 157–177.

Kumar, R., Rosen, M.A., 2011. Integrated collector-storage solar water heater with extended storage unit. Applied Thermal Engineering 31, 348–354.

Moghadam, H., Tabrizi, F.F., Sharak, A.Z., 2011. Optimization of solar flat collector inclination. Desalination 265, 107–111.

Rivera, W., Cardoso, M.J., Romero, R.J., 2001. Single-stage and advanced AHT operating with lithium bromide mixtures used to increase solar pond's temperature. Solar Energy Materials and Solar Cells 70, 321–333.

Singh, R., Tundee, S., Akbarzadeh, A., 2011. Electric power generation from solar pond using combined thermosyphon and thermoelectric modules. Solar Energy 85, 371–378.

Smyth, M., Eames, P.C., Norton, B., 2006. Integrated collector storage solar water heaters. Renewable and Sustainable Energy Reviews 10, 503–538.

Sun, H., Feistel, R., Koch, M., Markoe, A., 2008. New equations for density, entropy, heat capacity, and potential temperature of a saline thermal fluid. Deep-Sea Research I 55, 1304–1310.

Velmurugan, V., Srithar, K., 2007. Solar stills integrated with a mini solar pond-analytical simulation and experimental validation. Desalination 216, 232–241.

Velmurugan, V., Pandiarajan, S., Guruparan, P., Subramanian, L.H., Prabaharan, C.D., Srithar, K., 2009. Integrated performance of stepped and single basin solar stills with mini solar pond. Desalination 249, 902–909.